Biochemical and Biophysical Research Communications 443 (2014) 189–193

Contents lists available at ScienceDirect

Biochemical and Biophysical Research Communications

journal homepage: www.elsevier.com/locate/ybbrc

Pre-pore oligomer formation by *Vibrio cholerae* cytolysin: Insights from a truncated variant lacking the pore-forming pre-stem loop

Karan Paul, Kausik Chattopadhyay *

Department of Biological Sciences, Indian Institute of Science Education and Research (IISER) Mohali, Sector 81, SAS Nagar, Manauli 140306, Punjab, India

ARTICLE INFO

Article history:
Received 17 November 2013
Available online 26 November 2013

Keywords:
Vibrio cholerae cytolysin
Pore-forming toxin
Bacterial protein toxin

ABSTRACT

Vibrio cholerae cytolysin (VCC), a β-barrel pore-forming toxin (β-PFT), induces killing of the target eukaryotic cells by forming heptameric transmembrane β-barrel pores. Consistent with the β-PFT mode of action, binding of the VCC toxin monomers with the target cell membrane triggers formation of pre-pore oligomeric intermediates, followed by membrane insertion of the β-strands contributed by the pre-stem motif within the central cytolysin domain of each protomer. It has been shown previously that blocking of membrane insertion of the VCC pre-stem motif arrests conversion of the pre-pore state to the functional transmembrane pore. Consistent with the generalized β-PFT mechanism, it therefore appears that the VCC pre-stem motif plays a critical role toward forming the structural scaffold of the transmembrane β-barrel pore. It is, however, still not known whether the pre-stem motif plays any role in the membrane interaction process, and subsequent pre-pore structure formation by VCC. In this direction, we have constructed a recombinant variant of VCC deleting the pre-stem region, and have characterized the effect(s) of physical absence of the pre-stem motif on the distinct steps of the membrane pore-formation process. Our results show that the deletion of the pre-stem segment does not affect membrane binding and pre-pore oligomer formation by the toxin, but it critically abrogates the functional pore-forming activity of VCC. Present study extends our insights regarding the structure–function mechanism associated with the membrane pore formation by VCC, in the context of the β-PFT mode of action.

1. Introduction

β-Barrel pore-forming toxins (β-PFTs) constitute a unique class of membrane-damaging cytolytic protein toxins isolated from a wide array of pathogenic bacteria [1]. β-PFTs are, in general, secreted as water-soluble monomeric molecules, which upon interaction with the target cell membrane assemble into transmembrane oligomeric β-barrel channels, thus leading to the colloid osmotic lysis of the cells [1,2]. Generalized mechanism of membrane pore formation by β-PFTs proposes three intermediate steps in the process: (a) binding of the toxin monomers onto the cell membrane, (b) assembly of the membrane-bound monomers into transient, meta-stable, pre-pore oligomeric structures, (c) membrane insertion of the so called stem region from the toxin protomers to generate the transmembrane β-barrel pores [3–11]. In spite of such generalized scheme, individual members of the β-PFT family highlight significant deviations in terms of the mechanistic details of the process.

Vibrio cholerae cytolysin (VCC) is a prominent member in the family of β-PFTs [12,13]. VCC induces potent membrane-damaging cytolytic activity against wide range of target eukaryotic cells [14,15]. Cell killing activity of VCC is commonly attributed to its ability to form transmembrane oligomeric β-barrel channels in the membrane lipid bilayer of the target cells [12,16]. VCC is shown to form heptameric transmembrane β-barrel pores in the membrane lipid bilayer of erythrocytes as well as synthetic lipid vesicles [12]. Analysis of the structural models show that the central cytolysin domain of VCC harbors a pre-stem loop which remains packed within the protein structure in its water-soluble monomeric state (Fig. 1) [13]. In the process of transmembrane oligomeric pore formation, this pre-stem loop undergoes conformational change, comes out of the VCC structure, and inserts into the membrane lipid bilayer. Contribution of the pre-stem loops from the seven toxin protomers generates the stem region of the transmembrane β-barrel pore of VCC (Fig. 1) [12]. Covalent locking of the 'pre-stem' configuration via engineered disulfide linkage was found to arrest the toxin in an abortive pre-pore oligomeric state on the membrane, thus blocking functional transmembrane pore formation [17]. It therefore suggests that the conformational rearrangement and membrane insertion of the pre-stem region are crucial for conversion of the pre-pore state to the functional pore structures for VCC, as consistent with the generalized β-PFT mode of action. However, it is still not known whether the presence of the pre-stem motif in the VCC molecular structure

Abbreviations: VCC, *Vibrio cholerae* cytolysin; PFT, pore-forming toxin; FRET, fluorescence resonance energy transfer; CD, circular dichroism.

* Corresponding author. Fax: +91 0172 2240124.
E-mail address: kausik@iisermohali.ac.in (K. Chattopadhyay).

0006-291X/$ - see front matter © 2013 Elsevier Inc. All rights reserved.
http://dx.doi.org/10.1016/j.bbrc.2013.11.078

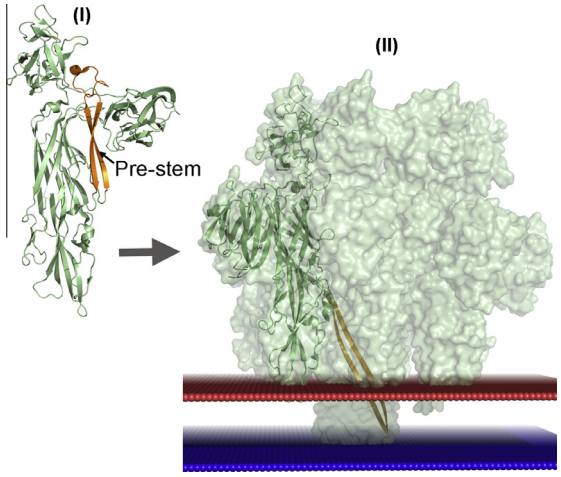

Fig. 1. Structural models showing the mechanism of membrane pore formation by VCC. Water-soluble monomeric form of VCC (I) binds to the target membrane and assemble into the heptameric transmembrane β-barrel pore (II). The pre-stem loop structure is shown in orange. One of the seven protomers in the VCC oligomer structure is highlighted. (For interpretation of the references to color in this figure legend, the reader is referred to the web version of this article.)

serves any critical role toward membrane binding and subsequent pre-pore structure formation. Since the pre-stem region contributes to generate the transmembrane segment of the β-barrel pore, it is worth testing whether the pre-stem loop is involved in making initial contacts of the VCC molecule with the membrane lipid bilayer, thus contributing toward the membrane binding step of the toxin. Analysis of the VCC oligomer structure highlights that a significant extent of the inter-protomer interactions are mediated by the residues within the transmembrane stem region of the protein [12]. Therefore, it also needs to be validated whether the pre-stem motif is critical to regulate the pre-pore oligomer formation step of the membrane-bound VCC protein. In order to address these issues, in the present study we have characterized a truncated variant of VCC deleting the pre-stem motif. Using this mutant form of VCC, we have specifically explored the effect of physical absence of the pre-stem structure on the following aspects of VCC mode of action: (a) structural integrity of the protein, (b) membrane binding, (c) oligomer formation, (d) membrane insertion, and (e) functional membrane pore formation.

2. Materials and methods

2.1. Protein expression and purification

Mature form of the wild type VCC protein was expressed and purified as described previously [18–20]. Nucleotide sequence encoding the VCC mutant deleting the pre-stem region (encompassing residues 281–322 of the VCC precursor, Pro-VCC [13]) was constructed by polymerase chain reaction (PCR)-based method. The pre-stem region was swapped with a short flexible linker sequence of Gly-Gly-Ser. The recombinant protein was expressed and purified following the method as described for VCC. Purity of the proteins were analyzed by SDS–PAGE/Coomassie staining. Protein concentrations were determined by monitoring absorbance at 280 nm, using theoretically calculated extinction coefficients of the proteins from their corresponding amino acid compositions.

2.2. Intrinsic tryptophan fluorescence and far-UV circular dichroism (CD) spectroscopy

Protein intrinsic tryptophan fluorescence spectra were recorded in a Fluoromax-4 (Horiba Scientific, Edison, NJ), with an excitation wavelength at 290 nm, using 250 nM protein concentration.

Far-UV CD spectra were recorded on a Chirascan spectropolarimeter (Applied Photophysics, Leatherhead, Surrey, UK) using 5 mm pathlength quartz cuvette. Protein concentrations were in the range 0.75–1 μM.

2.3. Assay of hemolytic activity

Hemolytic activity of the VCC variants (100 nM) against human erythrocytes was monitored as described previously [20]. Briefly, lysis of erythrocytes was measured by monitoring the decrease in turbidity (corresponding to OD_{650}) of the erythrocyte suspension in PBS [20 mM sodium phosphate, 150 mM sodium chloride, pH 7.4].

2.4. Flow cytometry

A flow cytometry-based assay was used to monitor binding of the VCC variants (75 nM) with human erythrocytes (10^6 cells), using a FACSCalibur (BD Biosciences) flow cytometer, as described previously [19].

2.5. Assay with liposome

Asolectin-cholesterol (1:1 weight ratio) liposome with or without trapped calcein were prepared as described previously [19]. For diphenylhexatriene (DPH)-labelled Asolectin-cholesterol liposome preparation, liposome suspension in PBS was incubated with DPH (DPH:liposome weight ratio of 1:200) for 1 h at 25 °C.

A pull-down assay was used to monitor binding and oligomerization of the VCC variants in the Asolectin-cholesterol liposome. Briefly, 1 μM protein in 1 ml PBS was incubated with 50 μg of liposome for 1 h at 25 °C, protein–liposome complex was pelleted by ultracentrifugation at 105,000g, pellet fraction was washed with PBS, and analyzed by SDS–PAGE/Coomassie staining. For BS^3 (bis[sulfosuccinimidyl] suberate; Thermo Pierce) cross-linking of pre-pore oligomer, protein–lipid complex was pelleted by ultracentrifugation, washed with PBS, resuspended in PBS containing 5 mM BS^3, and incubated for 1 h at 25 °C. The reaction was stopped by the addition of 150 mM Tris–HCl (pH 8.0), pelleted at 105,000g, and analyzed by SDS–PAGE/Coomassie staining.

Calcein-release assay was performed following the method described previously [19], using Perkin-Elmer LS 55 spectrofluorimeter. 1 μM protein was incubated in presence of 100 μg calecein-trapped Asolectin-cholesterol liposome in 2 ml reaction volume. Calcein fluorescence was measured at 520 nm upon excitation at 488 nm, using excitation and emission slit widths of 2.5 nm and 2.5 nm, respectively. The 100% calcein release was measured by treating liposome with 6 mM sodium deoxycholate.

Fluorescence resonance energy transfer (FRET) from tryptophan residue in protein to DPH incorporated in Asolectin-cholesterol liposome was monitored using a Perkin-Elmer LS 55 spectrofluorimeter. Tryptophan-to-DPH FRET signal was monitored by recording fluorescence at 470 nm upon excitation at 290 nm, with excitation and emission slit widths of 2.5 nm and 5 nm, respectively. 100 μg of DPH-labelled liposome was incubated with 1 μM protein in 2 ml reaction volume. Data were corrected by subtracting the reading obtained from DPH-labelled liposome without protein treatment.

2.6. Structural models

Structural coordinates of VCC were acquired from the Protein Data Bank (PDB) (VCC monomer structure was generated using the PDB structural coordinate 1XEZ; PDB structural coordinate 3O44 was used for the VCC oligomer). Structural model of the VCC oligomer in the membrane lipid bilayer was generated in

the OPM server found online (http://opm.phar.umich.edu/server.php). Protein structure models were represented using PyMOL [DeLano WL, The PyMOL Molecular Graphics System (2002) found online (http://pymol.org)].

3. Results and discussion

3.1. Structural integrity of the recombinant VCC mutant having truncation of the pre-stem region

In order to explore the role of the pre-stem loop in the structure–function mechanism of VCC, we constructed a truncated variant of VCC (ΔPS-VCC) lacking the pre-stem region within the cytolysin domain of the protein (Fig. 2A and B). In order to test the overall structural integrity of the truncated variant, we monitored intrinsic tryptophan fluorescence emission profile of the ΔPS-VCC protein. The intrinsic tryptophan fluorescence emission maximum of the truncated protein showed marginal red shift as compared to that of the wild type protein (Fig. 2C). Tryptophan fluorescence emission maxima of the proteins are determined by the contributions from all the tryptophan residues located at distinct environments within the protein structures. Therefore, marginal difference in the tryptophan fluorescence emission maximum of the VCC mutant could be explained by the fact that the ΔPS-VCC protein lacked one tryptophan residue located within the pre-stem region of the wild type toxin (11 tryptophan residues in wild type VCC versus 10 tryptophan residues in ΔPS-VCC). Whatsoever, the intrinsic tryptophan fluorescence profile of ΔPS-VCC suggested that the truncation of the pre-stem loop did not drastically affect the tryptophan environments, and therefore, the global tertiary structural organization of the protein. We also assessed the secondary structural organization of the ΔPS-VCC mutant by monitoring its far-UV CD spectrum, which showed a decreased ellipticity signal at 217 nm region (Fig. 2D). Once again, this could be explained by the fact that ΔPS-VCC lacked two β-strands corresponding to the pre-stem loop structure. Altogether, the intrinsic tryptophan fluorescence emission and the far-UV CD profile of ΔPS-VCC suggested that the removal of the pre-stem region did not affect the overall structural integrity of the protein.

3.2. ΔPS-VCC binds to the target membranes but does not induce membrane permeabilization

As depicted by the structural models, pre-stem region of the VCC molecule plays the most critical role in the process of transmembrane β-barrel pore formation. As shown in the heptameric pore structure of VCC [12], pre-stem loop from each of the toxin protomers inserts into the core of the membrane lipid bilayer to generate the stem regions that constitute the major structural scaffold for the transmembrane β-barrel pore (Fig. 1). Based on such model, physical truncation of the pre-stem region would be expected not to allow formation of the functional transmembrane pore. Consistent with such notion, ΔPS-VCC exhibited severely compromised membrane-damaging cytolytic activity against human erythrocytes (Fig. 3A). At a concentration of 100 nM, the truncated protein could not induce any lytic activity against human erythrocytes, when incubated for 1 h at 25 °C, (Fig. 3A). We employed a flow cytometry-based assay to test whether truncation of the pre-stem region could affect the binding of the mutant protein toward human erythrocytes. Our result showed that ΔPS-VCC displayed overall similar binding ability to human erythrocytes, as compared to that of the wild type VCC toxin (Fig. 3B). We also tested and compared the membrane-damaging activity of ΔPS-VCC and wild type VCC against Asolectin-cholesterol liposome using a standard calcein-release assay. As reported earlier [19], VCC shows potent membrane-damaging activity against Asolectin-cholesterol liposome, presumably due to the formation of the functional transmembrane β-barrel pores. Consistent with this, wild type VCC induced prominent calcein release from the Asolectin-cholesterol liposome, when tested with 1 μM protein concentration for 1 h at 25 °C (Fig. 3C). In contrast, the ΔPS-VCC mutant could not trigger any significant extent of liposome membrane permeabilization, when tested under the identical experimental condition (Fig. 3C). Consistent with the erythrocyte-binding data, a pull down-based assay also confirmed an efficient association of ΔPS-VCC with the liposome membrane (Fig. 3D). These data, altogether, suggested that the truncation of the pre-stem loop indeed abrogated the membrane-damaging pore-forming activity of the VCC variant, without compromising the binding ability of the mutant protein toward the target membranes.

3.3. Pre-pore oligomer formation by ΔPS-VCC

We tested the ability of ΔPS-VCC to form SDS-stable oligomeric assembly in the membrane lipid bilayer of liposome vesicles, a prominent signature of the transmembrane oligomeric pore structures formed by the archetypical β-PFTs including VCC. Our result showed that the ΔPS-VCC protein could associate with the Asolectin-cholesterol liposome, but did not form any SDS-stable oligomer in the liposome membrane (Fig. 3D). We also wanted to check whether ΔPS-VCC could form any SDS-labile pre-pore oligomeric assembly upon association with the liposome membrane. We used

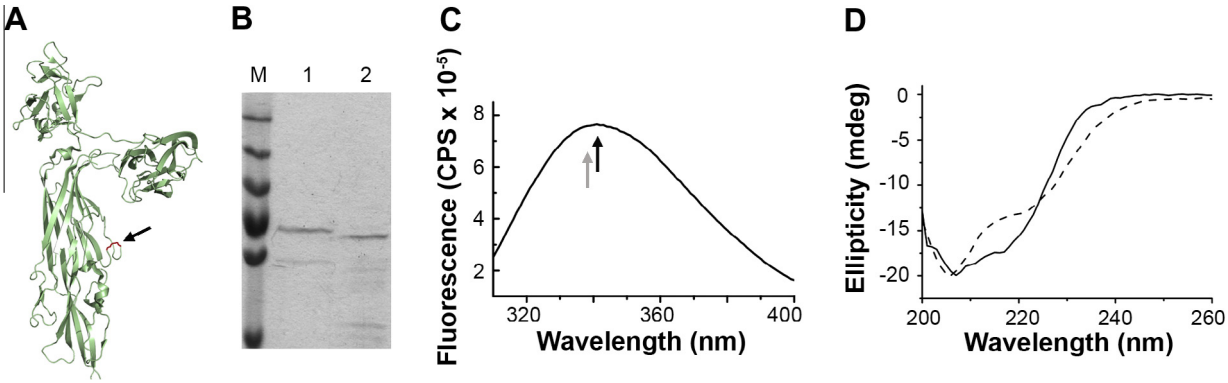

Fig. 2. (A) Representation of the ΔPS-VCC structural model. Deletion of the pre-stem loop via swapping with a three-residue linker (Gly-Gly-Ser) is shown in red and marked with an arrow. (B) SDS–PAGE/Coomassie staining profile of purified form of VCC (lane 1) and ΔPS-VCC (lane 2). Lane M, protein standards. (C) Intrinsic tryptophan fluorescence emission profile of ΔPS-VCC. Intrinsic tryptophan fluorescence emission maxima of ΔPS-VCC and wild type VCC are indicated with black and grey arrows, respectively. (D) Far-UV CD spectra of wild type VCC (solid line) and ΔPS-VCC (broken line). (For interpretation of the references to color in this figure legend, the reader is referred to the web version of this article.)

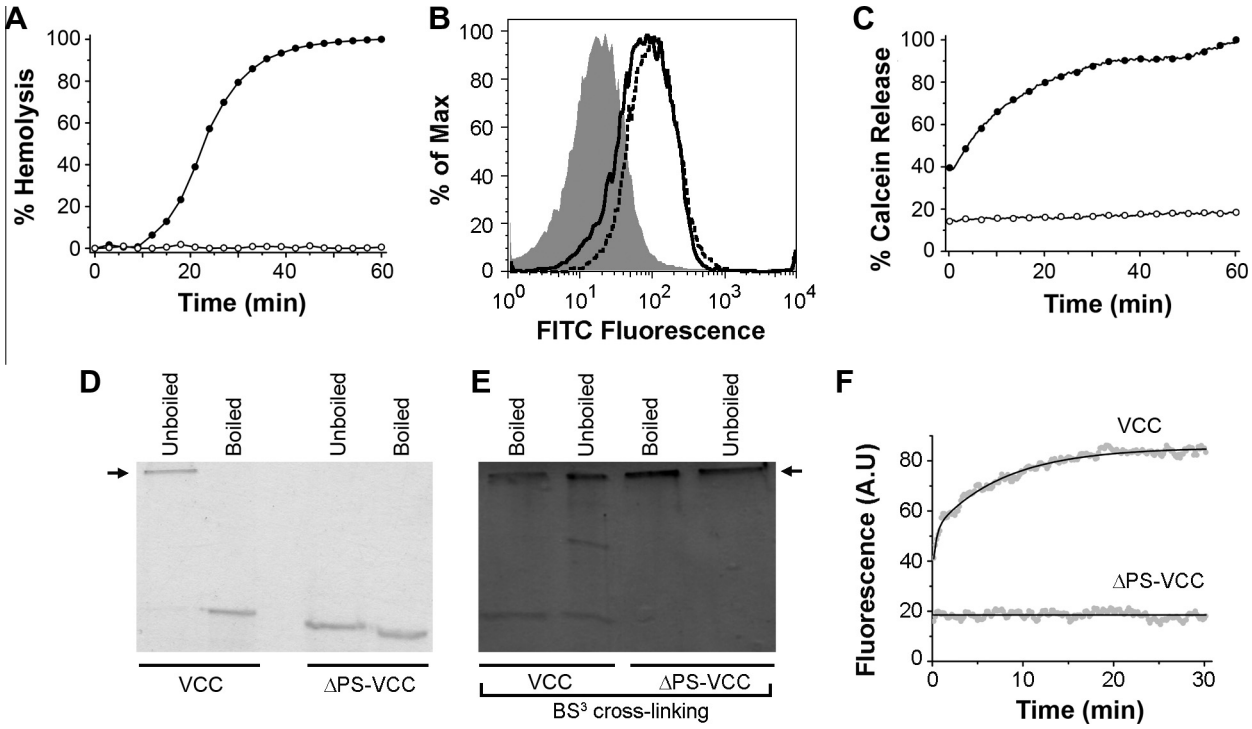

Fig. 3. (A) Hemolytic activity of wild type VCC (closed circle) and ΔPS-VCC (open circle) against human erythrocytes. (B) Binding of wild type VCC (solid line) and ΔPS-VCC (dashed line) with human erythrocytes, as determined by the flow cytometry-based assay. Shaded curve, control. (C) Membrane permeabilization effect of wild type VCC (closed circle) and ΔPS-VCC (open circle) against Asolectin-cholesterol liposome, as monitored by estimating the release of calcein from within the liposome vesicles. (D) Binding and SDS-stable oligomer formation in Asolectin-cholesterol liposome. Proteins were incubated in presence of the liposome vesicles, protein–liposome complexes were pelleted, dissolved in SDS–PAGE sample buffer with or without boiling, and were analyzed by SDS–PAGE/Coomassie staining. Samples without boiling showed SDS-stable oligomer formation by wild type VCC in the liposome membrane, whereas membrane-bound ΔPS-VCC did not form any SDS-stable oligomer. SDS-stable oligomer of wild type VCC is marked with an arrow. (E) BS^3 cross-linking of SDS-labile pre-pore oligomer of ΔPS-VCC formed in the Asolectin-cholesterol liposome membrane. Protein sample was incubated in presence of liposome, liposome-bound proteins were pelleted, subjected to BS^3 cross-linking, and was analyzed by SDS–PAGE/Coomassie staining. Wild type VCC was included as control. Cross-linked oligomers are indicated with an arrow. (F) Insertion of the pre-stem loop of wild type VCC into the membrane lipid bilayer of Asolectin-cholesterol liposome, as monitored by the tryptophan-to-DPH FRET. Membrane insertion of the pre-stem loop triggered increased fluorescence of the membrane-embedded DPH, presumably due to an efficient FRET from the Trp318 located within the pre-stem motif. ΔPS-VCC did not exhibit such FRET response due to the absence of the pre-stem structure.

the cross-linking agent BS^3 to covalently trap any oligomeric assembly formed by the ΔPS-VCC mutant in presence of the Asolectin-cholesterol liposome. Interestingly, the ΔPS-VCC mutant showed formation of oligomeric structures that could be trapped by BS^3-mediated cross-linking (Fig. 3E), suggesting that the truncation of the pre-stem region did not affect the ability of the protein to form SDS-labile pre-pore oligomeric assembly in the liposome membrane.

3.4. Abortive membrane insertion step for ΔPS-VCC

We confirmed abortive membrane insertion step for ΔPS-VCC due to its inability to contribute the pore-forming stem region. For this we employed a qualitative FRET-based assay where we monitored changes in the DPH fluorescence (incorporated into the hydrophobic core of the membrane lipid bilayer) upon excitation of the protein tryptophan fluorescence, during interaction of the VCC variants with the liposome membrane. In case of wild type VCC, out of its 11 tryptophan residues, one is located within the pre-stem region at position 318. In the process of the membrane insertion of the pre-stem region, this Trp318 would come into close proximity of the membrane-bound DPH fluorophore, thus resulting in an increased FRET signal (Fig. S1). In case of ΔPS-VCC, absence of the pre-stem structure encompassing the Trp318 residue would be expected to abolish the abovementioned FRET process. Consistent with such notions, incubation of wild type VCC with the DPH-labelled Asolectin-cholesterol liposome exhibited prominent increase in the tryptophan-to-DPH FRET signal, whereas ΔPS-VCC did not show any significant increase in the FRET profile (Fig. 3F).

In sum, in the present study, we explored the implication(s) of the pre-stem motif for the structure–function mechanism of VCC. Our study altogether extended our insights regarding the membrane pore formation process of VCC in the context of the generalized β-PFT mode of action.

Acknowledgments

This wok was supported by a grant from the Department of Biotechnology (DBT), India (DBT Grant No. BT/PR13350/BRB/10/751/2009). We also thank IISER Mohali for financial support.

We thank Dr. Arunika Mukhopadhaya of IISER Mohali for assistance with the analysis of the flow cytometry data.

Appendix A. Supplementary data

Supplementary data associated with this article can be found, in the online version, at http://dx.doi.org/10.1016/j.bbrc.2013.11.078.

References

[1] J.E. Alouf, M.R. Popoff, The Comprehensive Sourcebook of Bacterial Protein Toxins, Academic Press, 2006.

[2] I. Iacovache, M. Bischofberger, F.G. van der Goot, Structure and assembly of pore-forming proteins, Curr. Opin. Struct. Biol. 20 (2010) 241–246.

[3] I. Iacovache, F.G. van der Goot, L. Pernot, Pore formation: an ancient yet complex form of attack, Biochim. Biophys. Acta (BBA) – Biomembr. 1778 (2008) 1611–1623.
[4] M. Gonzalez, M. Bischofberger, L. Pernot, F. van der Goot, B. Frêche, Bacterial pore-forming toxins: the (w)hole story?, Cell Mol. Life Sci. 65 (2008) 493–507.
[5] S.J. Tilley, H.R. Saibil, The mechanism of pore formation by bacterial toxins, Curr. Opin. Struct. Biol. 16 (2006) 230–236.
[6] A.P. Heuck, R.K. Tweten, A.E. Johnson, Beta-barrel pore-forming toxins: intriguing dimorphic proteins, Biochemistry 40 (2001) 9065–9073.
[7] B. Walker, O. Braha, S. Cheley, H. Bayley, An intermediate in the assembly of a pore-forming protein trapped with a genetically-engineered switch, Chem. Biol. 2 (1995) 99–105.
[8] B. Walker, M. Krishnasastry, L. Zorn, H. Bayley, Assembly of the oligomeric membrane pore formed by Staphylococcal alpha-hemolysin examined by truncation mutagenesis, J. Biol. Chem. 267 (1992) 21782–21786.
[9] H. Bayley, L. Jayasinghe, M. Wallace, Prepore for a breakthrough, Nat. Struct. Mol. Biol. 12 (2005) 385–386.
[10] A. Valeva, M. Palmer, S. Bhakdi, Staphylococcal alpha-toxin: formation of the heptameric pore is partially cooperative and proceeds through multiple intermediate stages, Biochemistry 36 (1997) 13298–13304.
[11] L. Song, M.R. Hobaugh, C. Shustak, S. Cheley, H. Bayley, J.E. Gouaux, Structure of staphylococcal alpha-hemolysin, a heptameric transmembrane pore, Science 274 (1996) 1859–1866.
[12] S. De, R. Olson, Crystal structure of the *Vibrio cholerae* cytolysin heptamer reveals common features among disparate pore-forming toxins, Proc. Natl. Acad. Sci. USA 108 (2011) 7385–7390.
[13] R. Olson, E. Gouaux, Crystal structure of the *Vibrio cholerae* cytolysin (VCC) pro-toxin and its assembly into a heptameric transmembrane pore, J. Mol. Biol. 350 (2005) 997–1016.
[14] T. Honda, R.A. Finkelstein, Purification and characterization of a hemolysin produced by *Vibrio cholerae* biotype El Tor: another toxic substance produced by cholera vibrios, Infect. Immun. 26 (1979) 1020–1027.
[15] Y. Ichinose, K. Yamamoto, N. Nakasone, M.J. Tanabe, T. Takeda, T. Miwatani, M. Iwanaga, Enterotoxicity of El Tor-like hemolysin of non-O1 *Vibrio cholerae*, Infect. Immun. 55 (1987) 1090–1093.
[16] A. Zitzer, I. Walev, M. Palmer, S. Bhakdi, Characterization of *Vibrio cholerae* El Tor cytolysin as an oligomerizing pore-forming toxin, Med. Microbiol. Immunol. 184 (1995) 37–44.
[17] S. Lohner, I. Walev, F. Boukhallouk, M. Palmer, S. Bhakdi, A. Valeva, Pore formation by *Vibrio cholerae* cytolysin follows the same archetypical mode as {beta}-barrel toxins from gram-positive organisms, FASEB J. 23 (2009) 2521–2528.
[18] K. Paul, K. Chattopadhyay, Unfolding distinguishes the *Vibrio cholerae* cytolysin precursor from the mature form of the toxin, Biochemistry 50 (2011) 3936–3945.
[19] K. Paul, K. Chattopadhyay, Single point mutation in *Vibrio cholerae* cytolysin compromises membrane pore-formation mechanism of the toxin, FEBS J. 279 (2012) 4039–4051.
[20] A.K. Rai, K. Paul, K. Chattopadhyay, Functional mapping of the lectin activity site on the beta-prism domain of *Vibrio cholerae* cytolysin: implications for the membrane pore-formation mechanism of the toxin, J. Biol. Chem. 288 (2013) 1665–1673.